Electronic Supplementary Material (ESI) for Chemical Communications.

Trifunctional Integrated DNA Based Universal Sensing Platform for Detection of Diverse Biomolecules in One-pot Isothermal Exponential Amplification Mode

Yun-Xi Cui[1,2,†], Xue-Nan Feng[1,†], Xiao-Yu Li[1], Yu-Peng Zhang[1], An-Na Tang[1], De-Ming Kong[1,2,*]

[1] State Key Laboratory of Medicinal Chemical Biology, Tianjin Key Laboratory of Biosensing and Molecular Recognition, Research Centre for Analytical Sciences, College of Chemistry, Nankai University, Tianjin 300071, P R China

[2] Collaborative Innovation Center of Chemical Science and Engineering (Tianjin), Tianjin, 300071, P R China.

[†]These authors contribute equally

Experimental Section

Chemicals and apparatus

The poly-T (pT) DNA substrates (pT_{PNK}: 5′-TTTTTTTT-BHQ-TT(AP)TT-FAM-TTTTTTTT-3′-P; pT_{Dam}: 5′-TTTTTTTT-BHQ-TT(AP)TT-FAM-TTTTTTTTGGGGATCGGGTTTTCCCGATCCCC-3′-P) used in this project were synthesized and purified by GeneScript Biotech. Co. Ltd. (Nanjing, China). T4 polynucleotide kinase (T4 PNK), terminal transferase (TdT), Endonuclease IV (Endo. IV), Dam methyltransferase (Dam MTase), restriction endonuclease Dpn I, CpG methyltransferase M.SssI, bovine serum albumin (BSA), deoxyadenosine triphosphate (dATP) and corresponding buffer solutions were obtained from New England Biolabs (NEB, Beijing, China). All other chemicals without particular mentioned were applied in analytical grade and ordered from Solarbio (Beijing, China). All solutions for the reaction were prepared with ultrapure water which was purified by a Milli-Q water purification system(>18.25 MΩ cm^{-1}).

Gel electrophoresis imaging results were collected by a Gel Documentation System (Huifuxingye, Beijing, China). Fluorescence spectra were collected by Hitachi RF-5301 fluorescence spectrometer (Hitachi. Ltd., Japan). Real-time PARTIP assay was performed in a commercial StepOnePlus™ Real-Time PCR instrument (Applied Biosystems, USA).

T4 PNK activity assay

500 nM of pT_{PNK} substrate was mixed with 2 mM dATP, 10 U TdT, 5U Endo. IV in 1×TdT buffer (50 mM potassium acetate, 20 mM Tris-acetate, 10 mM magnesium acetate, pH 7.9) supplement with 200 μgmL^{-1} BSA and 250 μM $CoCl_2$ as a total volume of 25 μL. After adding different concentration of T4 PNK in, each mixture was incubated at 37 °C for 2h, followed with heating deactivation at 85°C for 20 min. For the end-point analytical mode, the fluorescence signal of the product was measured by the fluorescence spectrometer after the reaction. The excitation wavelength was set as 490 nm, and the emission spectrum from 500 nm to 650 nm was collected for further investigation. For the real-time analytical mode, the mixture was incubated in a StepOnePlus™ instrument and the fluorescence intensity was directly reported synchronously during the reaction proceeding.

Dam MTase activity assay

500 nM of pT_{Dam} substrate was mixed with 2 mM dATP, 10 U TdT, 5U Endo. IV and 5U DpnI in 1×TdT buffer supplement with 200 μg mL^{-1} BSA and 250 μM $CoCl_2$ as a total volume of 25 μL. After adding different concentrations of Dam MTase in, each mixture was incubated at 37 °C for 1h, followed with heating deactivation at 85°C for 20 min. For the end-point analytical mode, the fluorescence signal of the product was directly measured by the fluorescence spectrometer after the reaction. The excitation wavelength was set as 490 nm, and the emission spectrum from 500 nm to 650 nm was collected for further investigation. For the real-time analytical mode, the mixture was incubated in a StepOnePlus™ instrument and the fluorescence intensity was directly report synchronously during the reaction proceeding.

Gel electrophoresis assay

The products of PNK activity assay were analyzed using polyacrylamide gel electrophoresis (PAGE). The reactions with different components addition were performed at 37 °C for 2h. After reaction, 15 μL of the products were mixed with 3 μL 6×loading buffer. The mixture was loaded into a 10% polyacrylamide gel contained in 1×TAE buffer (40 mM Tris-acetic acid, 2 mM EDTA,

pH 8.0). The PAGE was performed under 120 V constant voltage at room temperature for 50 min. The gel was stained with ethidium bromide for 15 min. The stained gel was imaged using Gel Documentation Imaging System.

T4 PNK inhibitor assay

For the T4 PNK inhibitor assay, different concentration of $(NH_4)_2SO_4$ or Na_2HPO_4 were mixed with the reaction system and pre-incubated for a certain time. The reactions and the fluorescence measurement were similar as described above, all of the reaction time was keep at 37 °C for 3h, and the relative activities (R_A) of T4 PNK were calculated based on eqn (1):

$$R_A=(F_T-F_0)/(F_C-F_0) \quad (1)$$

where F_T, F_C, and F_0 represent the fluorescence intensity in the presence of different concentrations of inhibitors, in the absence of inhibitors and blank control without target enzyme, respectively. According to the fitting plots, the half maximal inhibition (IC_{50}) is defined as the concentration of the inhibitors applied to achieve a 50% relative activity.

Detection of T4 PNK activity in cell lysate

HeLa cells were first cultured in a humidified atmosphere of 95% air and 5% CO_2, at 37 °C in Dulbecco′s modified Eagle′s medium (DMEM, Gibco) supplemented with 1% penicillin-streptomycin (Gibco) and 10% fetal calf serum (Sijiqing, Beijing, China). Nucleoprotein extraction kits (Sangon Biotech, Shanghai, China) were applied to extract the cell lysate. The extracted cell lysate was applied for T4 PNK activity assay immediately or stored at -80 °C. The procedures of the analysis were similar as those described above except that cell lysate was added as an alternate of T4 PNK.

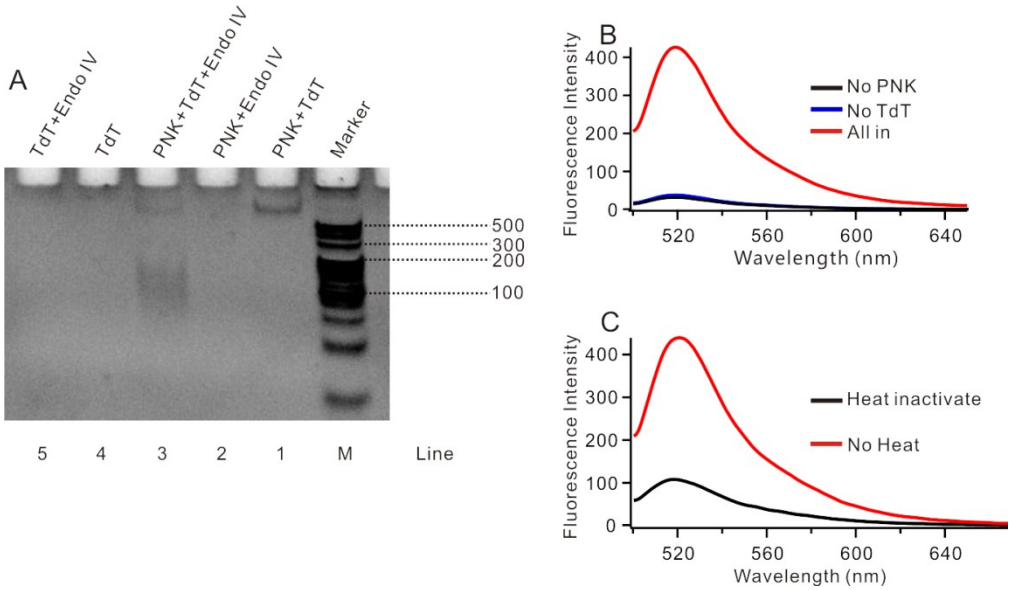

Figure S1: (A) The PAGE result of the sensing platform with different components adding in. line M: the markers, Lane 1: reaction with T4 PNK and TdT, no Endo. IV; Lane 2: with T4 PNK and Endo. IV, no TdT; Lane 3: with T4 PNK, TdT and Endo. IV; Lane 4:with TdT only; Lane 5: with TdT and Endo. IV, no T4 PNK. (B) The fluorescent spectra in response to the sensing platform with different components adding in. (C) The fluorescent spectra in response to the sensing platform with or without heating inactivity before the addition of the Endo. IV

Figure S2-S6 showing the results of the optimization of the working condition for PARTIP including the concentrations of BSA, pT_{PNK}, dATP, TdT, and Endo. IV. Comparing the signal-to-noise ratio under different conditions, we finally obtained the optimized reaction conditions of 500 nM of pT_{PNK}, 2mM dATP, 10 U TdT, 5 U Endo. IV and 200 mg mL^{-1} BSA in 1×TdT buffer (50 mM potassium acetate, 20 mM tris acetate, 10 mM magnesium acetate, pH 7.9) supplemented with 250mM $CoCl_2$ in a total volume of 25 mL.

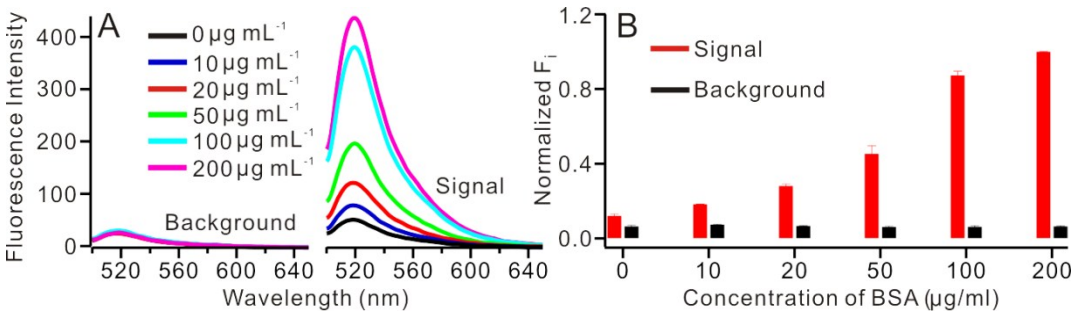

Figure S2: (A) Fluorescent spectra in response to different concentrations of BSA (B) Measurement of the fluorescence intensity at 520 nm of the spectra in response to different concentrations of BSA. The concentration of 200μg mL^{-1} shows a highest signal-to-noise ratio (S/N), the normalization was calculated based on setting the intensity of the signal at the optimal condition as 1.

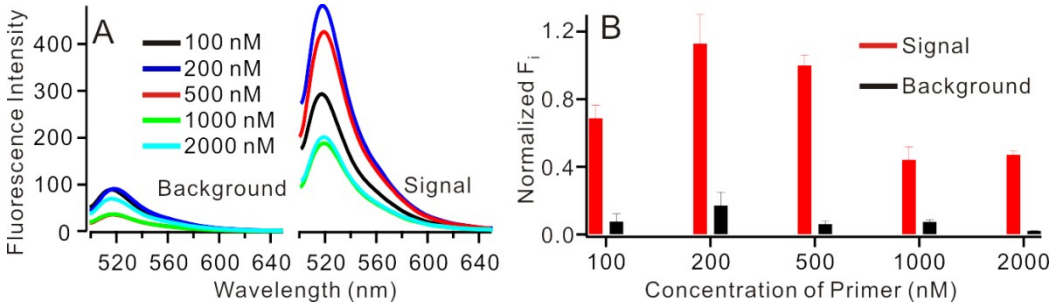

Figure S3: (A) Fluorescent spectra in response to different concentrations of pT_{PNK} substrate (B) Measurement of the fluorescence intensity at 520 nm of the spectra in response to different concentrations of pT_{PNK} substrate. The concentration of 500 nM pT_{PNK} substrate shows a highest signal-to-noise ratio (S/N), the normalization was calculated based on setting the intensity of the signal at the optimal condition as 1.

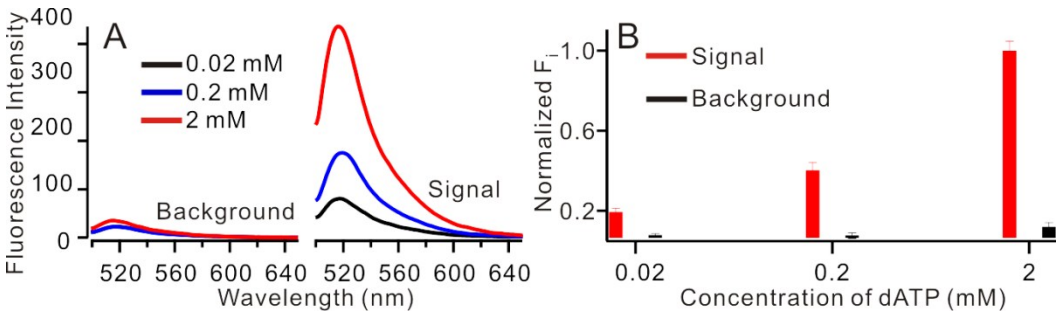

Figure S4: (A) Fluorescent spectra in response to different concentrations of dATP (B) Measurement of the fluorescence intensity at 520 nm of the spectra in response to different concentrations of dATP. The concentration of 2 mM dATP shows a highest signal-to-noise ratio (S/N), the normalization was calculated based on setting the intensity of the signal at the optimal condition as 1.

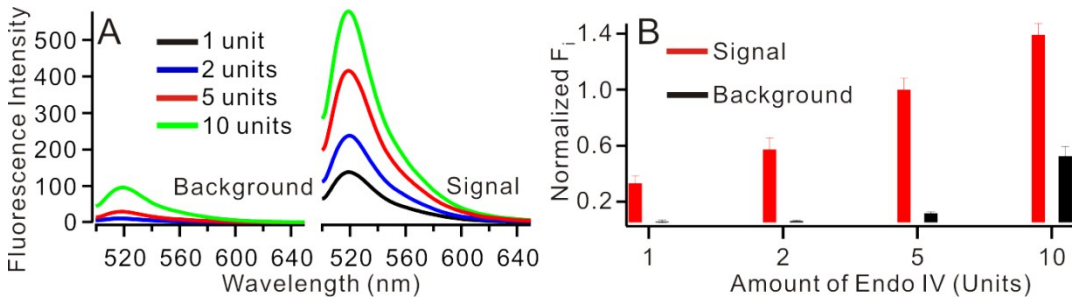

Figure S5: (A) Fluorescent spectra in response to different amounts of Endo. IV (B) Measurement of the fluorescence intensity at 520 nm of the spectra in response to different amounts of Endo. IV. The amount of 5U Endo. IV shows a highest signal-to-noise ratio (S/N), the normalization was calculated based on setting the intensity of the signal at the optimal condition as 1.

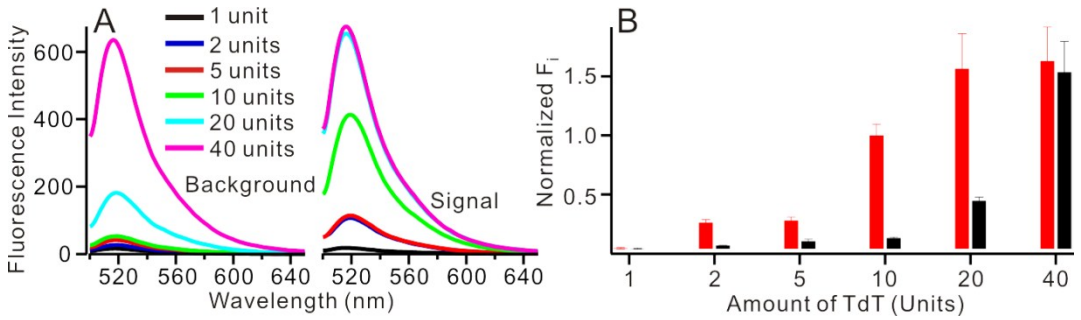

Figure S6: (A) Fluorescent spectra in response to different amounts of TdT (B) Measurement of the fluorescence intensity at 520 nm of the spectra in response to different amounts of TdT. The amount of 10U TdT shows a highest signal-to-noise ratio (S/N), the normalization was calculated based on setting the intensity of the signal at the optimal condition as 1.

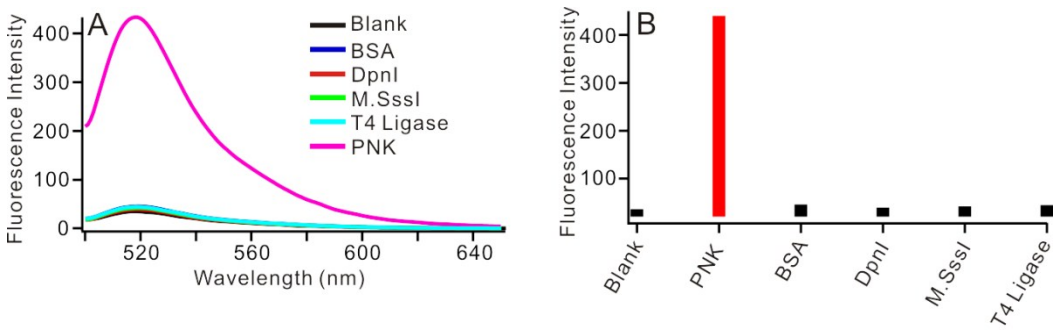

Figure S7: Selectivity assay. (A) Fluorescent spectrum in response to different enzymes or proteins, the concentration of the BSA is 200 μg mL^{-1}, the concentration of the enzyme DpnI, M.SssI, T4 Ligase are 1 U mL^{-1}, the concentration of T4 PNK is 0.1 U mL^{-1}. (B) Measurement of the fluorescence intensity at 520 nm of the spectra in response to different enzymes or proteins.

We employed BSA, endonuclease DpnI, methyltransferase M.SssI, and T4 ligase as the competitive proteins and enzymes. As shown in Fig. S7, the increase of fluorescence signal was observed only in the presence of T4 PNK, revealing the excellent selectivity of the PARTIP towards the target.

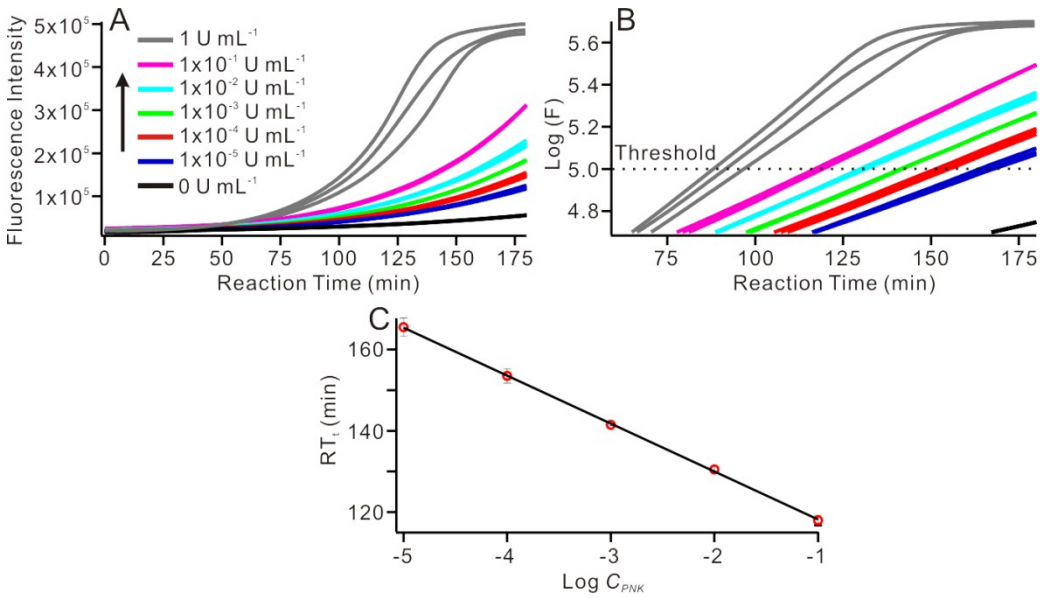

Figure S8: The PNK activity assay by RT-qPCR. (A) Fluorescence-Time (F-RT) plots and (B) Log(F)-RT plot obtained in real-time detection mode under different concentrations of PNK in a range of 1×10^{-5} to 1 U mL^{-1}. (C) The linear relationship between the RT_t values (threshold is set as 5.0) and the logarithm of the concentrations of PNK from 1×10^{-5} to 1×10^{-1} U mL^{-1}.

Fluorescence intensity (F) *vs* reaction time (RT) curves were collected at different PNK concentrations from10^{-5} to 1 U mL^{-1}. In logarithmic scale, log(F)–RT curves were calculated based on the F–RT plots (Fig. S8B). Then the RT_t values, the reaction time when the log(F) reached the set threshold, were calculated from the log(F)-RT plots. As shown in Fig S8C, a linear relationship was constructed between the RT_t values and the concentrations of PNK in a wide range of 10^{-5} to 10^{-1} U mL^{-1}. The linear regression equation was calculated as RT_t=212.8-23.6×logC_{PNK}, with a correlation coefficient of 0.999.

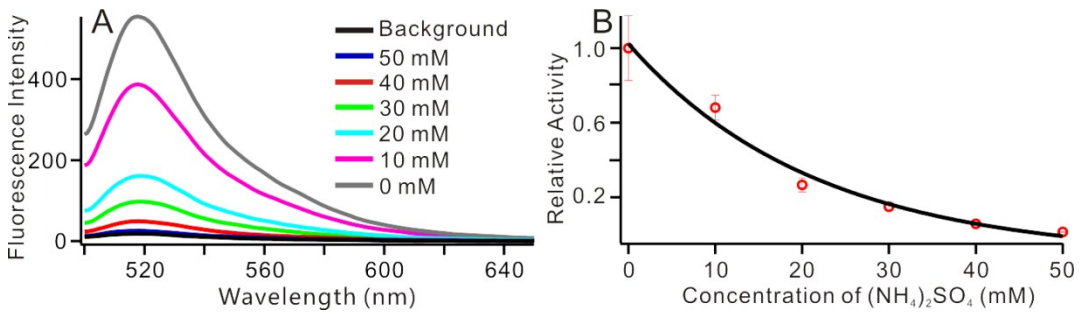

Figure S9: Inhibitor assay by $(NH_4)_2SO_4$ (A) Fluorescent spectra in response to different concentrations of $(NH_4)_2SO_4$ (B) Variance of the relative activity of PNK in response to different concentrations of $(NH_4)_2SO_4$. The concentration of PNK is 0.1 U mL^{-1}.

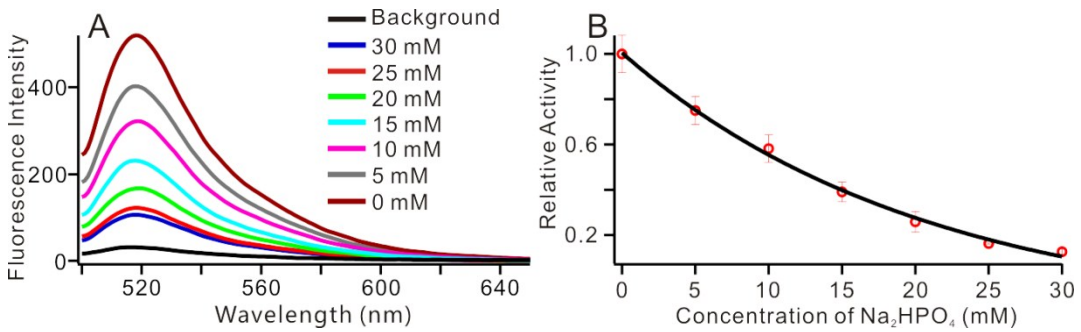

Figure S10: Inhibitor assay by Na_2HPO_4 (A) Fluorescent spectra in response to different concentrations of Na_2HPO_4 (B) Variance of the relative activity of PNK in response to different concentrations of Na_2HPO_4. The concentration of PNK is 0.1 U mL^{-1}.

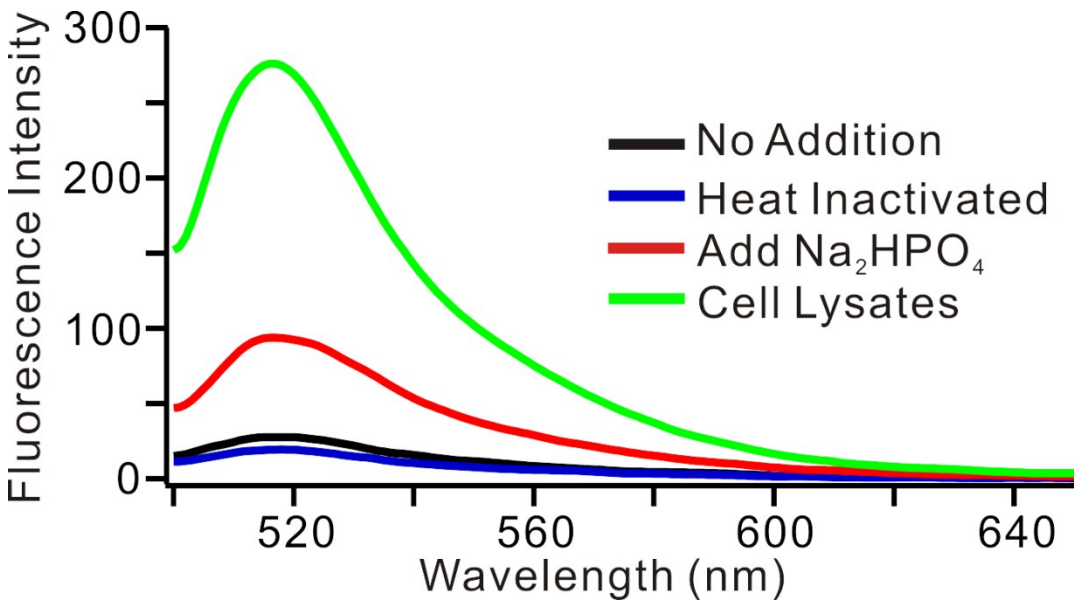

Figure S11: Fluorescent spectra in response to HeLa cell lysates, heating-inactivated cell lysate, lysate pre-incubated with 20 mM Na_2HPO_4, and blank control.

As shown in Fig. S11, the fluorescence intensity increased significantly with addition of HeLa lysate. Because such an enhancement was sharply decreased by addition of Na_2HPO_4, and almost disappeared after a deactivation treatment of the lysate at 95 °C for 20 minutes, it is verified that the cell lysate-triggered fluorescence intensity increase was really related with active PNK.

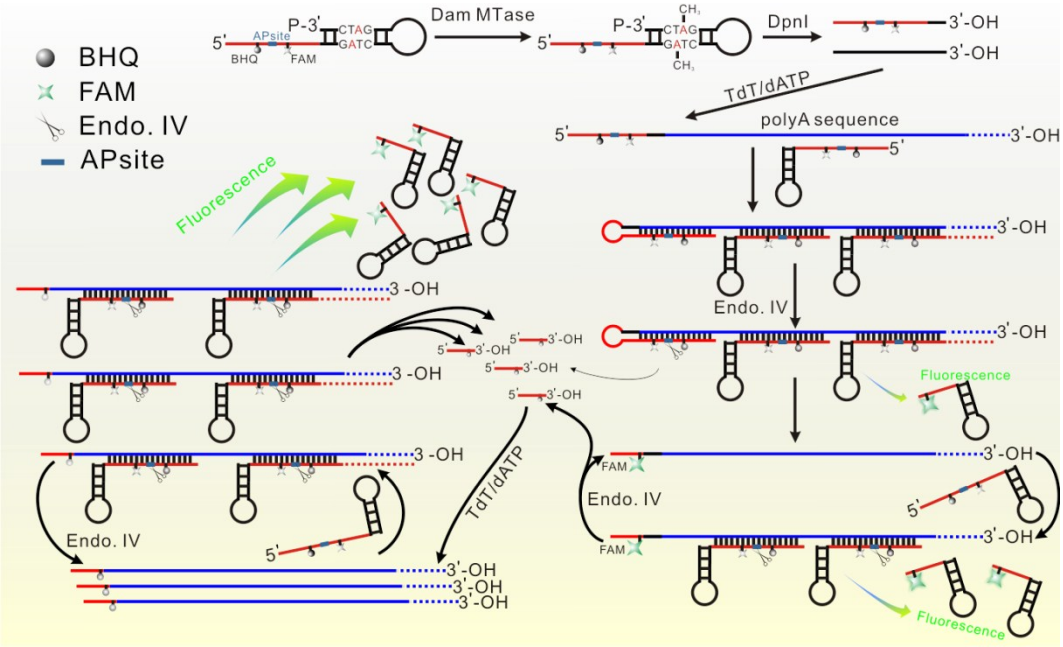

Figure S12: The mechanism of the Dam MTase-PARTIP. Briefly, the 5'-GATC-3' part located in a hairpin region will be recognized by Dam Methyltransferase, and the "A" (adenine) will be methylated to "mA" base. Then the DpnI can cleave the DNA substrate at the "mA" position, resulting two shorter pieces with exposed 3'-OH end. The TdT can elongate the DNA from the 3'-OH end, using dATP as the material of the polymerization, the product of the elongation is a long tail with pA sequence. Next, the pT part of the substrate may hybridize with the pA tail, and the Endo. IV can cleave the substrate at the pre-set AP site position. So the FAM labelled close to a BHQ will be separate from the quencher, and the fluorescence signal will be recovered.

We extended previously used pT_{PNK} strand with a hairpin structure, which contain a palindromic sequence of 5′-G-A-T-C-3′/5′-C-T-A-G-3′ in the stem region. The obtained pT_{Dam} strand was also modified with a 3′-P end which block the elongation reaction catalyzed by TdT. In the presence of Dam MTase, the adenines (A) in the palindromic sequence will be methylated, and the methylated adenines can be subsequently cleaved by endonuclease DpnI. The cleavage of the pT_{Dam} strand would generate two short DNA pieces with exposed 3′-OH, thus initiating the signal amplification reactions in the presence of TdT and Endo. IV, and achieving the highly sensitive quantitation of Dam MTase activity.

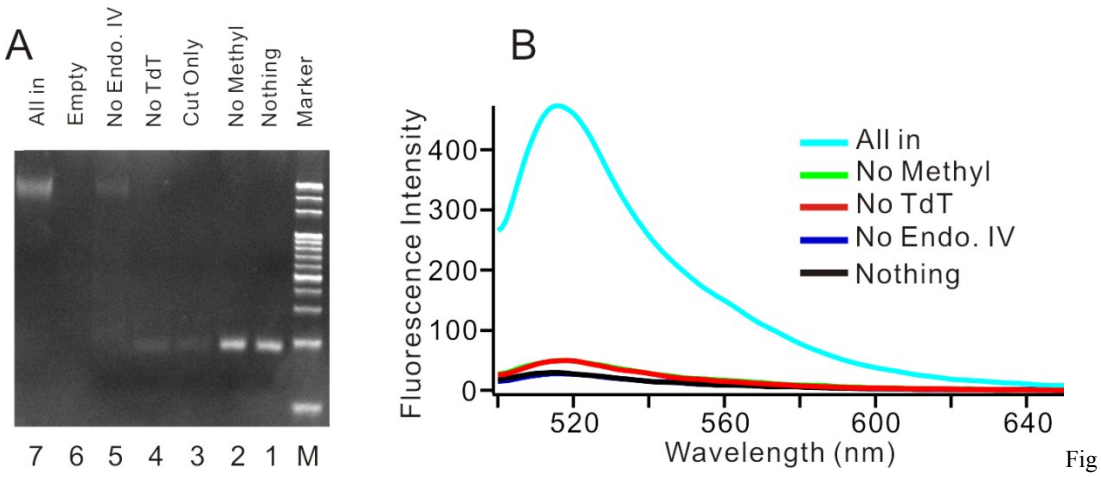

Figure S13: (A) The PAGE result of the Dam MTase-PARTIP with different components adding in. Line M: the markers, Line 1: original substrate with no enzyme; Line 2: without Dam MTase; Line 3: with Dam MTase and DpnI only; Line 4: without TdT; Line 5: without Endo. IV; Line 6: empty control; Line 7: with all components. (B) The fluorescent spectra of the sensing systems with different components adding in.

In the presence of Dam MTase and DpnI, the band of pT_{Dam} much lighter, indicating the destruction of the hairpin structure (Fig. S13A, Lane 3). Next, TdT may elongate the cut substrate so a band with slower migration rate according to ~500 nt was appeared (Fig. S13A, Lane 5). With further addition of Endo. IV, the ~500 nt band was much brighter (Fig. S13A, Lane 7), suggesting that the exponential amplification reaction proceeded. Also, the fluorescence result revealed that the signal amplification processes could be initiated only in the presence of Dam MTase (Fig. S13B).

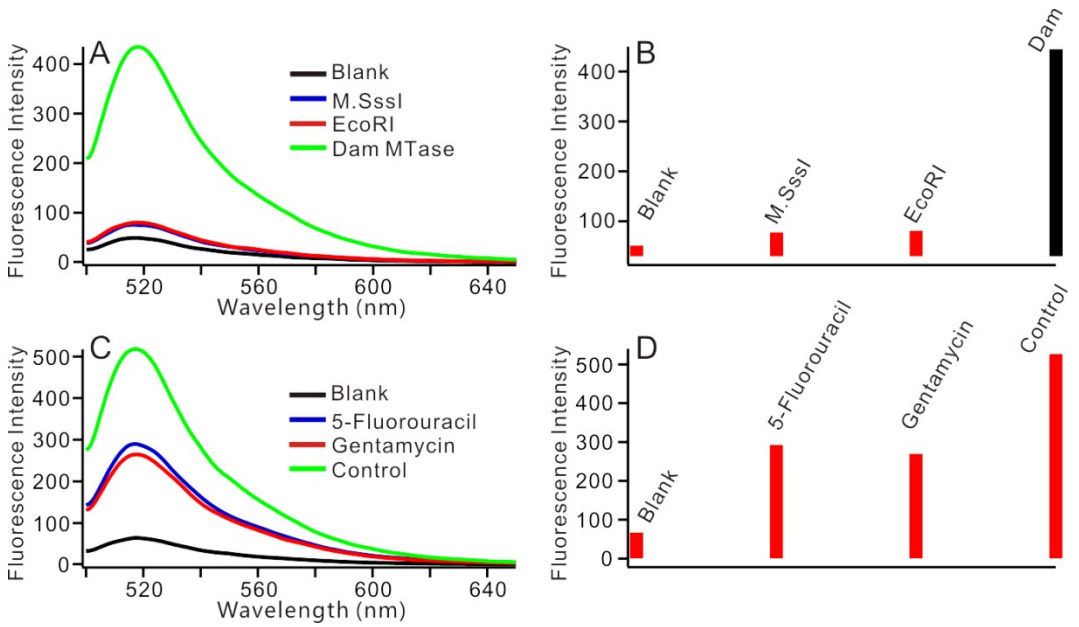

Figure S14: Selectivity of the Dam MTase-PARTIP and its application in inhibitor assay of Dam MTase.(A) Fluorescent spectra in response to different enzymes, the concentration of the enzyme M.SssI and EcoRI are 10 U mL^{-1}, the concentration of dam MTase is 4 U mL^{-1}. (B) Measurement of the fluorescence intensity at 520 nm of the spectra in response to different enzymes. (C) Fluorescent spectra in response to 5-fluorouracil and gentamycin, the concentration of Dam MTase employed was 10 U mL^{-1}. (D) Measurement of the fluorescence intensity at 520 nm of the spectra in response to5-fluorouracil and gentamycin.

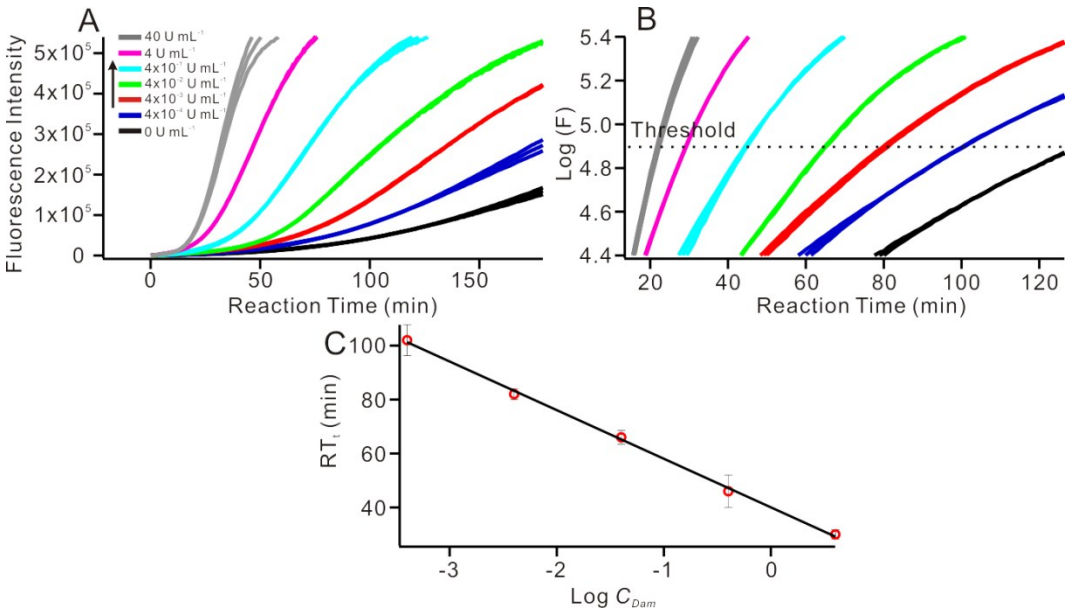

Figure S15: The Dam MTase activity assay in real-time detection mode. (A) Fluorescence-Reaction Time (F-RT) plot and (B) Log(F)-RT plot obtained in real-time detection mode under different concentration of Dam MTase in a range of 4×10^{-4} to 40 U mL^{-1}. (C) The linear relationship between the RT_t value and the logarithm of the concentration of Dam MTase from 4×10^{-4} to 4 U mL^{-1} using 4.9 as the threshold.

A linear relationship was obtained on the logarithmic scale in the range of 4×10^{-4} to 4 U mL^{-1}. The linear regression equation was calculated as $RT_t=40.0-18.0\times\log C_{Dam}$, with a correlation coefficient of 0.999.

Table S1. Comparison of several PNK detection methods

Method	Detection limit (U mL^{-1})	Cell analysis	Reference
Rolling circle amplification-induced chemiluminescence	2.20×10^{-4}	Yes	S1
Au nanoparticle assisted single molecular fluorescence	9.77×10^{-5}	Yes	S2
Magnetic separation conjugated RCA	4.36×10^{-5}	No	S3
λ exonuclease assisted paper-based fluorescence assay	1×10^{-4}	Yes	S4
Dual enzyme assisted real-time assay	1×10^{-5}	Yes	S5
Au nanoparticle based electrochemical assay	7.76×10^{-4}	No	S6
Total integrated system	3.5×10^{-6}	Yes	This work

Reference:

(1) Tang, W.; Zhu, G. C.; Zhang, C. Y. *Chem. Commun.***2014**, *50*, 4733.

(2) Wang, L. J.; Zhang, Q.; Tang, B.; Zhang, C. Y. *Anal.Chem.***2017**, *89*, 7255.

(3) Li, X.; Xu, X. W.; Song, J.; Xue, Q. W.; Li, C. Z.; Jiang, W. *Biosens. Bioelectron.***2017**, *91*, 631.

(4) Zhang, H.; Zhao, Z.; Lei, Z.; Wang, Z. *Anal. Chem.***2016**, *88*, 11358.

(5) Li, X.-Y.; Du, Y.-C.; Pan, Y.-N.; Su, L.-L.; Shi, S.; Wang, S.-Y.; Tang, A.-N.; Kim, K.; Kong, D.-M. *Chem. Commun.***2018**, *54*, 13841.

(6) Cui, L.; Li, Y.; Lu, M.; Tang, B.; Zhang, C. Y. *Biosens. & Bioelectron.***2018**, *99*, 1.